RSC Advances

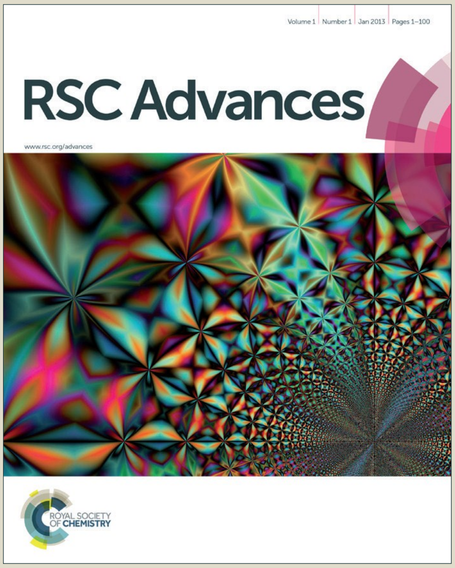

ROYAL SOCIETY OF CHEMISTRY

www.rsc.org/advances

Mechanically synthesized SiO_2–Fe metal matrix composite for effective dechlorination of aqueous 2-chlorophenol: the optimum of the preparation conditions

Yunfei Zhang[a,b], Bo Yang[b,*], Jinhong Fan[a,*], and Luming Ma[a]

[a] National Engineering Research Center for Urban Pollution Control, State Key Laboratory of Pollution Control and Resources Reuse, College of Environmental Science and Engineering, Tongji University, 200092 Shanghai, P. R. China

[b] Department of Environmental Engineering, College of Chemistry and Environmental Engineering, Shenzhen University, 518060 Shenzhen, P.R. China

---

* Corresponding author. Tel.: +86-755-2673 2904; fax: +86-755-2653 6141.

E-mail address: boyang@szu.edu.cn (B. Yang), jinhongfan@tongji.edu.cn (J.H. Fan)

Abstract: In this study, the synthesized abrasives−reinforced metal matrix composites (MMCs) with a microscale size by ball milling (BM) could achieve highly active and stable dechlorination efficiency for aqueous 2-chlorophenol (2-CP). The preparation process of this composite via BM was optimized to obtain high degradation efficiency, especially for the effect of the abrasives including B_4C, SiC, α-Al_2O_3, SiO_2, Fe_3O_4 and Na_2SO_4. The results showed that the hardness of the abrasives in the Fe−based MMCs was closely related with their dechlorination performance. Subsequently, the optimal abrasive, i.e. SiO_2 was further investigated for its proper milling conditions with zero-valent iron (ZVI) particles including SiO_2 size, SiO_2 loading, milling time, and the dosage of the process control agent (PCA). Additionally, the influence of other metal categories including Al and Si was also investigated for dechlorination; and their low reaction efficiencies were closely related with their passivating film. Finally, the longevity test suggested that the decreased reactivity of the SiO_2−Fe MMC during the storage in air could be recovered when consecutively used, mainly due to the promoting effects of inherent structure of SiO_2−Fe MMC with the Fe/C and Fe/SiO_2 interfaces, as well as the effective regeneration of the reactive sites by continuous iron dissolution.

Keywords: 2-chlorophenol; Abrasives; Ball milling; Dechlorination; Iron metal matrix composite; Process control agent.

1. Introduction

Recently, the zero-valent iron (Fe^0–ZVI) has been widely used for the reductive dechlorination of chlorinated organic compounds (COCs) under both laboratory and field conditions [1-4]. By using ZVI as electron donor, many chloralkanes and chlorinated alkenes can be rapidly reduced into non-toxic or low toxic chlorine-free hydrocarbons. Some environmental remediation fields in USA have utilized this reductive material to purify the water containing short-chain COCs. For example, when groundwater passed through the permeable reactive barriers constructed by zero-valent iron (FePRBs), the short-chain COCs in the water would be effectively degraded into hydrocarbons [5, 6]. However, the dechlorination rate for chlorinated aromatics is rather slow due to their recalcitrant properties, with half-lives of days or longer calculated by pseudo-first-order kinetics [7].

Lessening the size of Fe^0 particles to nanoscale is one approach to enhance the dechlorination activity of iron. The nano zero-valent iron (nZVI) has been found to present much higher reactivity than conventional iron particles because of its higher surface area and denser active sites from its nanostructure [7]. However, its preparation method usually entails the expensive sodium borohydride to reduce ferrous or ferric ion [1, 7] into ZVI. Moreover, nZVI particles are thermodynamically unstable in solution and tend to aggregate into micro to millimeter scale's particles [7]. Doping a second metal into iron, like Pd, Pt, Ni, and Cu, to form bimetallic catalyst is another approach to enhance the reactivity of iron [8-10]. This enhancement is due to the accelerated iron corrosion by bimetallic galvanic couple and the generation of highly active atomic H* with the doped metal as the catalyst. However, the preparation cost of bimetals and potential leaching of the second metal into groundwater restrict their widely application [11].

Recently, particulate-reinforced metal matrix composites (p−MMCs) have attracted considerable attention in industries application [12, 13]. Those p−MMCs are synthesized by embedding a reinforcing material (such as Si_3N_4, AlN, $A1_2O_3$, quartz sand) into a monolithic metal matrix to improve the raw material properties [14, 15]. Compared with the nZVI and bimetals, the preparation of the Fe-based p−MMCs was usually much more convenient and cost-effective, as a result of availability of relatively inexpensive reinforcements, and the development of various processing routes [16]. For example, as a single step process, ball milling (BM) is a convenient and practical technique to homogeneously distribute reinforcement into metal matrix [17]. On the other hand, in the field of environmental technology, BM could be also used to produce highly active metallic materials by repeated welding, fracturing, and rewelding of the solid materials [18]. For example, Xu et al. [8] recently utilized BM technique to prepare bimetallic Ni/Fe particles and used them to dechlorinate 4-chlorophenol in aqueous solution. As a result, Ni particles were dispersed homogeneously in Fe phase after BM and highly active and stable dechlorination efficiency was achieved by the ball-milled Ni/Fe particles. So, the use of BM to produce the Fe-based p−MMCs for the removal of environmental pollutants should be promising. However, to our knowledge, seldom such studies have been reported.

In this work, we attempted to directly prepare the ball-milled ZVI particles for dechlorination purpose only through mechanically adding abrasive without combining the second metal. This process actually provided a novel synthetic method of ZVI as the reductive material for the degradation of environmental pollutants. The performance of different reinforcement as abrasive was investigated by evaluating the dechlorination efficiency of the synthesized ZVI toward 2-chlorophenol. And the milling conditions were subsequently optimized. In addition, the dechlorination performances of other zero-valent metals (including Al and Si particles) using the above ball-milling technique were also explored. Finally, the longevity performance of the SiO_2−Fe MMC was evaluated.

2. Materials and methods

2.1. Materials

Fe (>99%, 100 mesh), Al (>99%, 100 mesh), Si (>99%, 100 mesh) and iron(II) sulfate heptahydrate ($FeSO_4 \cdot 7H_2O$) were purchased from Aladdin, Inc. Analytical-grade quartz sand (> 99%, 10~325 mesh), NaOH (98.0%), and HCl (36–38%) were obtained from Tianjing Tianli Chemical Reagent Co., Ltd., Tianjin Guangfu Technology Development Co., Ltd., and Dongguan Dongjiang Chemical Reagent Co., Ltd., respectively. Boron carbide (B_4C, >90%, 100 mesh) , Silicon carbide (SiC, 98.5%, 100 mesh) and α-Alumina (α-Al_2O_3, 99.99%, 100 mesh) were supplied by Sinopharm Chemical Reagent Co., Ltd. 2-CP (99.9%) and phenol (99.9%) were procured from AccuStandard, Inc. HPLC-grade methanol and ethanol were acquired from TEDIA Co. All solutions were prepared using water with a resistance of 18.2 MΩ from a Millipore-Q system.

2.2. SiO_2-Fe MMC Prepared by Ball Milling

BM was carried out with a planetary ball mill (QM-3SP04, Nanjing University Instrument Corporation) at a rotation speed of 550 rpm without inert gas protection. Stainless vials (100 mL) as grinding container were fitted with two different sizes of stainless steel balls: 16 large balls (Φ10 mm) and 100 small balls (Φ6 mm). For each BM process, the materials added into the vial included 156 g of steel balls and 5 g of metal and reinforcement mixture. Unless otherwise stated, the weight ratio of metal powder to reinforcement was 9:1. Ethanol (6%, *w/w*) served as a control agent during BM. To prevent spontaneous combustion of the energetic powder, the container was cooled down to room temperature before opening the container lid in air at the end of ball milling.

2.3. Characterization

The particle morphologies of the MMCs were characterized by scanning electron microscopy (SEM) (Hitachi S-3400N II). The BET surface areas (S_{BET}) of the samples were analyzed through nitrogen adsorption (NOVA 1200E). The size distribution of the SiO_2−Fe MMC was measured using a laser particle size analyzer (Mastersizer 3000, Malvern Instruments Ltd., UK).

2.4. Dechlorination of 2-CP and Analysis

Dechlorination was performed in a 100 mL three-neck flask attached with a pH meter (PHS-3C, Shanghai Precision & Scientific Instrument Co., Ltd.). A 50 mL aliquot of 2-CP solution with an initial pH=3.0 was added into the flask. Prior to reaction, 2 g of the milled powders was washed in 100 mL of H_2SO_4 solution (pH 1.0) for 10 min and rinsed three times with deionized water. Without drying, the washed SiO_2–Fe MMC particles were placed into the loosely capped flask, and the solution was continuously stirred at 220 rpm with a mechanical stirrer. All experiments were completed at room temperature (25 ± 2 ℃) and ambient pressure. The concentrations of 2-CP and phenol as products were measured using an HPLC system [14] (It is noted that no other further hydrogenation products such as cyclohexanone and cyclohexanol were found in GC-ECD analysis as reported in previous literature [19, 20]). Data were plotted as mean of duplicates, and error bars indicate deviation from the mean.

2.5. SiO_2-Fe MMC Stability and Reusability

In order to test the stability of the SiO_2−Fe MMC during storage, the SiO_2−Fe MMC was directly exposed to air at room temperature (25 ± 2 °C). Six consecutive dechlorination cycles using the same SiO_2−Fe MMC (with a dose of 40 g/L) was tested for estimate its reactivity toward 50 ppm 2-CP at initial pH=3.0 after storage for 10 days. Each cycle was conducted in a 50 mL serum bottle equipped with fresh 2-CP solution, an open-top screw cap, and PTFE-lined septa. After each cycle, the bottle was centrifuged at 5000 rpm for 5 min to separate the SiO_2−Fe particles from the aqueous phase. Subsequently, the used particles were rinsed with 50 mL deionized water; after centrifuged, the supernatant was emptied out. For each cycle, the reaction efficiencies for 2-CP removal were monitored and evaluated.

3. Results and Discussion

3.1. Effect of Abrasives

Different reinforcement materials (B_4C, SiC, α-Al_2O_3 and SiO_2) were milled with iron to investigate their effect on dechlorination efficiency of 2-CP. The Na_2SO_4 salt and the Fe_3O_4 oxide were also used as abrasives as comparison. As illustrated in Fig. 1, significantly higher dechlorination efficiency was achieved when using the reinforcement materials as abrasives. 78.2% remove efficiency was observed when iron milled with SiO_2. Even higher degradation efficiency was presented when employing B_4C, SiC and α-Al_2O_3, which could remove 99.1%, 98.7% and 98.7% of 2-CP during 120-min reaction, respectively. However, when iron milling with Fe_3O_4, no enhancements for 2-CP removal efficiency were observed compared with that of the iron milled without abrasives (11.6% and 13.6%, respectively). And as for Na_2SO_4, the remove efficiency was slightly higher, increased to 27.6%. The S_{BET} of the milled powders were also analyzed. As illustrated in Table 1, the observed dechlorination efficiency by those reactive materials agreed well with the trend of their surface area, i.e., B_4C−Fe ≈ SiC−Fe ≈ α-Al_2O_3−Fe > SiO_2−Fe > Na_2SO_4/Fe ≈ Fe_3O_4/Fe. Thus, the smaller iron particles could provide more active sites on the iron surface for 2-CP adsorption and reaction, thereby increasing the activity for 2-CP dechlorination [7].

Fig. 1

The above difference of S_{BET} should be attributed to the different cutting abilities of abrasives for iron particles, which was closely related with their hardness [21]. Yılma [22] suggested that the harder the abrasive was, the faster and deeper cutting action it would provide and more quickly the milled particles would be ground into small particles. Table 1 listed the hardness index of the concerned abrasives using Mohs' scale [23, 24], whose magnitudes were well corresponding to their surface area except Fe_3O_4. Within Mohs' scale from 1 to 10, B_4C, SiC and α-Al_2O_3 possess relatively higher values i.e., 9.5, 9.3~9.5 and 9.0, respectively, so their S_{BET} were the relatively high as shown in Table 1. In addition, SiO_2 (with a hardness of 7.0) system presented lower surface area than those of B_4C, SiC and α-Al_2O_3, which was also consistent with the order of hardness values, and so as for Na_2SO_4, which is 2.8.

Table 1

However, though Fe_3O_4 provided a higher hardness values as 6.0 than that of Na_2SO_4, it presented lower surface area and removal efficiency toward 2-CP. This was probably caused by the magnetic force between the Fe_3O_4 and iron particles [25]. During the milling, the Fe_3O_4 and iron particles were prone to aggregate together and resulted in the formation of surface-passivating oxide layers (Fe_3O_4) on iron surface [26]. So these oxide layers blocked the active sites on the iron surface and inhibited the dechlorination reaction. Additionally, previous studies [27] demonstrated that the sulfate-containing system would also increase the sorption capacity of the COCs on iron surface, thus increasing the subsequent 2-CP removal efficiency. As a result, using Na_2SO_4 as abrasives presented slightly higher removal efficiency than that of Fe_3O_4.

Based on above results, the reinforcement materials including B_4C, SiC, α-Al_2O_3 and SiO_2 are the appropriate abrasives to prepare highly efficient ZVI particles for the dechlorination of 2-CP. However, due to its low cost, SiO_2 was selected as the optimum abrasive in this system. Subsequently, the preparation conditions of the SiO_2–Fe MMC were further investigated in the following experiments.

3.2. Effect of SiO_2 Sizes and SiO_2 Loading

The reinforcement materials have important effects on the property of ball-milled material and the subsequent dechlorination efficiency, which provided a cutting action for iron in the milling process and also served as the interface for dechlorination reaction [14]. So, the effects of SiO_2 size and its loading on dechlorination efficiency were investigated. As illustrated in Fig. 2, the dechlorination efficiency increased with increasing the SiO_2 size. Generally, abrasives with relatively small size do not have a large cutting force, which is more suitable for grinding function to material polishing. So it was not favorable for effectively reducing the particle size of iron [21, 28]. Thus, lower removal efficiency for 2-CP appeared in the iron milled with smaller SiO_2 particles. Coronado et al. [29] also reported that the wear rate of α-Al_2O_3 for Fe increased with increasing abrasives sizes until reaching a critical particle size (about 116 μm). Therefore, relatively large size of SiO_2 (10~20 mesh) as abrasive presented higher forming performance of ZVI particles and dechlorination efficiency.

Fig. 2

Fig. 3 shows the dechlorination efficiency of 2-CP using the SiO_2–Fe MMC prepared by different SiO_2 loading. It indicates that, even adding small fraction of

SiO_2 (5%), the remove efficiency of 2-CP was significantly increased (from 16.2% to 82.6%). And the highest remove efficiency was achieved for milling with 10% SiO_2 loading. However, further increase in SiO_2 content led to a reduction of 2-CP remove efficiency (especially from 20% to 40%). In fact, it can be inferred that the dechlorination reaction should be mainly occurred at the quartz sand/iron interfaces [14]. In the reductive dechlorination reaction, the iron was the ultimate electron donor [30]. The introducing of quartz sand in the iron matrix was not only favorable for the formation of discontinuous iron phase, thus promoting the iron dissolution and subsequent dechlorination reaction. The uniform distribution of the quartz sand could also retard the reactivity drop for the SiO_2–Fe MMC by separating the iron precipitates from formation of the dense oxide layers. As a result, the dechlorination efficiency of 2-CP increased due to the formation of more reactive sites with increasing the SiO_2 loading from 0% to 10%. However, too much SiO_2 loading would decrease the available electrons transferred from ZVI to 2-CP since the excessive SiO_2 in SiO_2−Fe MMC decreased the proportion of iron as electron donor during dechlorination [31]. So, the 10% SiO_2 loading was the optimum adding ratio to prepare this MMC material for dechlorination. Therefore, the following studies adopted the 10% SiO_2 loading with a diameter of 10~20 mesh as ball-milling parameter.

Fig. 3

3.3. Effect of Milling Time and Amount of PCA

The BM is a solid-state powder processing involving repeated welding, fracturing, and rewelding of powder particles [18]. Process variables in this method especially milling time, PCA amount have great influences on the final structure and morphology of the powders [26, 32], so their influence on 2-CP dechlorination efficiency was investigated. As illustrated in Table 2, the dechlorination efficiency increased with increasing the milling time from 0 h to 4h. In the early stages of milling, the ductile iron particles tended to be deformed, whereas the brittle SiO_2 particles fractured into small particles; at this stage fracturing was dominant, the size of the milled powder became smaller. When longer time was applied, these flattened particles began to get cold welded together and form the aggregated particles. After a certain time of milling, the rate of welding is dynamically balanced with that of fracturing and the average particle size of the powders remains relatively unchanged [33]. On the other hand, previous studies have suggested the organic PCA tended to be decomposed into carbon with the proceeding of the milling and the addition of the quartz sand would accelerate the carbonization rate [34]. So, when iron and carbon particles are in contact, massive microscopic galvanic cells will be formed spontaneously between the iron (anode) and carbon (cathode), thus accelerating the iron dissolution and subsequent dechlorination reaction. Therefore, longer milling time benefited the carbonization of the PCA and the formation of smaller particle size [32], so the 2-CP dechlorination efficiency was improved due to the formation of more Fe–C galvanic cell and more active sites in SiO_2−Fe system [7, 14, 35]. In consideration of activity and cost, 3 h was used to prepare the SiO_2−Fe MMC particles.

Table 2

In addition, the effect of PCA dosage on the degradation of 2-CP were also investigated. As illustrated in Table 2, increasing the PCA dosage from 0% to 6% significantly increased the dechlorination efficiency; however, the dechlorination efficiency was decreased when further increasing its dosage from 6% to 10%. This phenomenon could be explained by the dual effect of the PCA served during the mechanical milling, i.e., (i) the carbon source and (ii) the lubricant. At the same milling time, higher PCA dosage was favorable for the formation of more Fe–C galvanic cells and promoted the following dechlorination reaction. However, when the dosage of PCA was larger than >6%, the dechlorination efficiency was decreased, probably because the milling time was not long enough to carbonize all PCA present. So, the remaining trapped PCA (ethanol) in the inherent structure of the MMC hindered the 2-CP adsorption and the subsequent dechlorination reaction [36]. On the other hand, the balance between cold welding and fracturing requires a certain amount of PCA [32, 34]. When the ethanol was less than 6 *wt*.%, such as 1, 2 or 4 *wt*.%, its amount was not sufficient enough to cover the surfaces of the powder particles. As a result, the powders tend to cold-weld into large particles in the milling process, which would decrease the dechlorination efficiency due to the decreased active sites [37]. However, an excess amount of PCA would decrease the effectiveness of ball-powder collisions. Because the lubricating effect of the PCA could make powder particles slide laterally easily during collision [38]. Therefore, the optimized milling conditions for synthesizing the SiO_2−Fe MMC were determined by milling for 3 h with a 6% PCA addition. The formed powder was microscale-sized with a diameter of 20.4 μm (D50, median diameter) in the above milling condition (Fig. 4).

Fig. 4

3.4. Effect of Zero Valent−Metal Categories

As the common zero−valent metal, Al and Si were also used as reduction material to remove environmental pollutants [39, 40]. So the effect of these metals on 2-CP degradation efficiency was subsequently investigated. As illustrated in Table 3, SiO_2−Si and SiO_2−Al could not effectively degrade 2-CP in the 120-min of test period. But for SiO_2−Fe, 91.8% of 50 ppm 2-CP could be removed within 120-min reaction. The surface morphologies of the different MMCs were also characterized as shown in Fig. 5. The SiO_2−Al particles had an obviously smooth surface and clearly chopped sharp edges. It also indicated that the SiO_2−Si processed much smaller sizes compared with those of SiO_2−Al and SiO_2−Fe. While, most of SiO_2−Fe particles were intertwined into kinks-like structure.

Table 3

Fig. 5

The possible explanation for above dechlorination performance could be attributed to the nature difference of the passivating film on the surface of MMCs. For SiO_2−Al and SiO_2−Si, the corrosion dissolution of Al^0 and Si^0 was inhibited by their dense passivating film on the surface and, concomitantly, hindering the subsequent dechlorination reaction [40, 41]. This could be proved by the fact that no obvious H_2 bubble was observed in the reaction for both SiO_2−Al and SiO_2−Si system and a relatively constant pH value (~5.8 and ~ 6.0 for SiO_2−Al and SiO_2−Si system, respectively) appeared after 5-min reaction. As for Al, the native alumina film reformed easily by the reversible hydrolysis and condensation reactions even pretreated before by acid [41]. And given that the solution stable at ~5.8, the surface aluminum oxide layers are extremely stable at this condition based on our previous studies [42, 43]. Similar as that of Al, the Si surface was also covered by the fairly stable hydrogen-terminated silicon (H-Si) and silicon oxide, which was hardly dissolved in acid conditions [40]. However, the Fe could maintain continuous dissolution even at weak acidity or even neutral surroundings, which was attributed to the relatively weak interaction between hydroxides/oxides and Fe surface as well as the intertwined structure of the SiO_2−Fe (Fig. 5) [42, 44, 45]. Johnson et.al [46] and Farrel et.al [47] reported that the continuous remove of contaminants could still be achieved even at initial pH 5.8 and 6.2, respectively. So, 2-CP could be effectively removed by SiO_2−Fe in this system.

3.5 Stability and Reusability of the SiO_2−Fe MMC

The stability of the SiO_2−Fe MMC prepared at the above optimized conditions was evaluated to study whether its high activity would sustain during storage, which is essential to practical application. Although the dechlorination efficiency for those particles stored in air for 10 days was decreased from 91.8% to 72.4% in the first run, its reactivity could be recovered when consecutively used. For example, both the 2-CP removal percent were still more than 95% from the second to the third cycle. And the dechlorination efficiency at the sixth run could still achieve 71.0% and 60.5% for the fresh prepared and after stored particles, respectively. The relatively stable performance of SiO_2−Fe MMC for dechlorination in the above tests should be attributed to its inherent structure. Unlike the core–shell structure of the common bimetal materials [48-50], The SiO_2−Fe MMC was constituted by numerous iron-carbon interface and quartz sand/iron interface in its relative uniform system. Those disperse interfaces could provide the driving force for sustained iron corrosion in water. Thus, the reactivity could be effectively remained due to the continuously regeneration of the active sites. Therefore, the SiO_2−Fe MMC could provide better longevity and practicability than the core–shell bimetals.

4. Conclusion

In this work, the preparation conditions of the reinforcement/metal MMCs were optimized by evaluating their reactivity to dechlorinate 2-CP in aqueous solution. The effect of the abrasives on dechlorination efficiency was investigated including B_4C, SiC, α-Al_2O_3, SiO_2, Fe_3O_4 and Na_2SO_4. It was found that the B_4C−Fe, SiC−Fe, α-Al_2O_3−Fe and SiO_2−Fe MMC could effectively degrade 2-CP, which possessed relative high hardness for the abrasive used. However, SiO_2 was selected as the optimal abrasive due to its low cost. Subsequently, it was further optimized for the preparation conditions of SiO_2−Fe MMC, which finally included 10~20 mesh SiO_2, 10% of SiO_2 loading, milling for 3 h and 6% PCA addition. Under the optimized preparation condition, the synthetic SiO_2−Fe MMC achieved a degradation efficiency of 91.8% 2-CP (0.389 mM) in 3 h using a dosage of 40g/L at initial pH=3.0. The influence of other metal categories including Al and Si was also investigated for dechlorination; and their low reaction efficiencies were closely related with their passivating film. Additionally, the micorsized SiO_2−Fe MMC could recover its reactivity after storage in air, which could avoid the deactivation the bimetallic system with core-shell structure or the aggregation of nZVI particles. Therefore, it would benefit the potential application of SiO_2−Fe MMC in the permeable reactive barrier technologies for the treatment of COC-contaminated groundwater.

Acknowledgments

We thank the National High-Tech Research and Development Program of China (863 Program, 2013AA062705), the National Natural Science Foundation of China (21547011, 21177089, 51108330), and the Shenzhen Science and Technology Project for Fundamental Research (JCYJ20150324141711622, JCYJ20150529164656097).

References

1. C. M. Kocur, A. I. Chowdhury, N. Sakulchaicharoen, H. K. Boparai, K. P. Weber, P. Sharma, M. M. Krol, L. Austrins, C. Peace and B. E. Sleep, *Environ Sci Technol*, 2014, **48**, 2862-2869.
2. Y. L. Jiao, C. C. Qiu, L. H. Huang, K. X. Wu, H. Y. Ma, S. H. Chen, L. M. Ma and D. L. Wu, *Applied Catalysis B: Environmental*, 2009, **91**, 434-440.
3. R. A. Doong, S. Saha, C. H. Lee and H. P. Lin, *RSC Advances*, 2015, **5**, 90797-90805.
4. X. S. Zha, L. Ma and Y. Liu, *RSC Advances*, 2016, **6**, 16323-16330.
5. L. M. Ma and W. X. Zhang, *Environ Sci Technol*, 2008, **42**, 5384-5389.
6. Y. Furukawa, J. W. Kim, J. Watkins and R. T. Wilkin, *Environ Sci Technol*, 2002, **36**, 5469-5475.
7. R. Cheng, J. L. Wang and W. X. Zhang, *J Hazard Mater*, 2007, **144**, 334-339.
8. F. Y. Xu, S. B. Deng, J. Xu, W. Zhang, M. Wu, B. Wang, J. Huang and G. Yu, *Environ Sci Technol*, 2012, **46**, 4576-4582.
9. B. W. Zhu and T. T. Lim, *Environ Sci Technol*, 2007, **41**, 7523-7529.
10. Y. Lv, Z. Niu, Y. Chen and Y. Hu, *RSC Advances*, 2016, **6**, 20357-20365.
11. M. Zhang, D. B. Bacik, C. B. Roberts and D. Zhao, *Water Res*, 2013, **47**, 3706-3715.
12. L. Zhong, F. Ye, Y. Xu and J. Li, *Mater Design*, 2014, **54**, 564-569.
13. T. Wang, M. Shozaki, M. Yamamoto and A. Kagawa, *Mater Design*, 2015, **66**, 498-503.

14. Y. Zhang, B. Yang, Y. Han, C. Jiang, D. Wu, J. Fan and L. Ma, *Chemosphere*, 2016, **146**, 308-314.

15. S. Sulaiman, M. Sayuti and R. Samin, *J Mater Process Technol*, 2008, **201**, 731-735.

16. I. Ibrahim, F. Mohamed and E. Lavernia, *J Mater Sci*, 1991, **26**, 1137-1156.

17. A. Pakseresht, H. A. Baghbaderani and R. Yazdani-Rad, *T Indian I Metals*, 2016, **69**, 1007-1014.

18. S. l. Li, W. l. Yan and W. x. Zhang, *Green Chem*, 2009, **11**, 1618-1626.

19. C. Molina, A. Pizarro, J. Casas and J. Rodriguez, *Applied Catalysis B: Environmental*, 2014, **148**, 330-338.

20. L. Yin, J. Niu, Z. Shen and J. Chen, *Environ Sci Technol*, 2010, **44**, 5581-5586.

21. R. Gåhlin and S. Jacobson, *Wear*, 1999, **224**, 118-125.

22. N. G. Yılmaz, *Rock Mech Rock Eng*, 2011, **44**, 725-733.

23. D. R. Lide, ed., *CRC handbook of chemistry and physics*, CRC Press, Boca Raton, 2000, pp 4-154.

24. G. V. Samsonov, *Handbook of the Physicochemical Properties of the Elements*, Ifi/Plenum New York-Washington, New York-Washington, 1968, pp 432.

25. R. Hong, T. Pan, Y. Han, H. Li, J. Ding and S. Han, *J Magn Magn Mater*, 2007, **310**, 37-47.

26. E. Ganjeh, H. Khorsand and S. Shahsavar, *Mater Lett*, 2015, **143**, 144-147.

27. J. F. Devlin and K. O. Allin, *Environ Sci Technol*, 2005, **39**, 1868-1874.

28. B. Moshtaghioun, A. Monshi, M. Abbasi and F. Karimzadeh, *International Journal of Refractory Metals and Hard Materials*, 2011, **29**, 645-650.

29. J. Coronado and A. Sinatora, *Wear*, 2011, **271**, 1804-1812.

30. T. Li and J. Farrell, *Environ Sci Technol*, 2000, **34**, 173-179.

31. Y. H. Liu, F. L. Yang, P. L. Yue and G. H. Chen, *Water Res*, 2001, **35**, 1887-1890.

32. L. Lu and Y. Zhang, *J Alloy Compd*, 1999, **290**, 279-283.

33. L. Kollo, M. Leparoux, C. R. Bradbury, C. Jäggi, E. Carreño-Morelli and M. Rodríguez-Arbaizar, *J Alloy Compd*, 2010, **489**, 394-400.

34. V. G. Surkov, A. K. Golovko and O. I. Lomovsky, Khimiya v interesakh ustoichivogo razvitiya, 2010, 18, 165-170.

35. B. P. Chaplin, M. Reinhard, W. F. Schneider, C. Schüth, J. R. Shapley, T. J. Strathmann and C. J. Werth, *Environ Sci Technol*, 2012, **46**, 3655-3670.

36. D. Rath and K. Parida, *Ind Eng Chem Res*, 2011, **50**, 2839-2849.

37. B. Long, H. Zuhailawati, M. Umemoto, Y. Todaka and R. Othman, *J Alloy Compd*, 2010, **503**, 228-232.

38. L. Shaw, J. Villegas, H. Luo, M. Zawrah and D. Miracle, *Metallurgical and Materials Transactions A*, 2003, **34**, 159-170.

39. W. Liu, H. Zhang, B. Cao, K. Lin and J. Gan, *Water Res*, 2011, **45**, 1872-1878.

40. R. A. Doong, K. T. Chen and H. C. Tsai, *Environ Sci Technol*, 2003, **37**, 2575-2581.

41. B. C. Bunker, G. C. Nelson, K. Zavadil, J. Barbour, F. Wall, J. Sullivan, C. F. Windisch, M. Engelhardt and D. R. Baer, *The Journal of Physical Chemistry B*, 2002, **106**, 4705-4713.

42. B. Yang, Y. Zhang, S. Deng, G. Yu, Y. Lu, J. Wu, J. Xiao, G. Chen, X. Cheng and L. Shi, *Chem Eng J*, 2013, **234**, 346-353.

43. B. Yang, J. X. Zhang, Y. Y. Zhang, S. B. Deng, G. Yu, J. H. Wu, H. Zhang and J. H. Liu, *Chem Eng J*, 2014, **250**, 222-229.

44. Z. Zhang, N. Cissoko, J. J. Wo and X. H. Xu, *J Hazard Mater*, 2009, **165**, 78-86.

45. Y. F. Su, C. Y. Hsu and Y. H. Shih, *Chemosphere*, 2012, **88**, 1346-1352.

46. T. L. Johnson, M. M. Scherer and P. G. Tratnyek, *Environ Sci Technol*, 1996, **30**, 2634-2640.

47. J. Farrell, M. Kason, N. Melitas and T. Li, *Environ Sci Technol*, 2000, **34**, 514-521.

48. T. Tabakova, L. Ilieva, P. Petrova, A. Venezia, G. Avdeev, R. Zanella and Y. Karakirova, *Chem Eng J*, 2015, **260**, 133-141.

49. C. H. Lin, Y. H. Shih and J. MacFarlane, *Chem Eng J*, 2015, **262**, 59-67.

50. C. Luo, Z. Chen, D. Wu and L. Ma, *Chem Eng J*, 2014, **241**, 376-383.

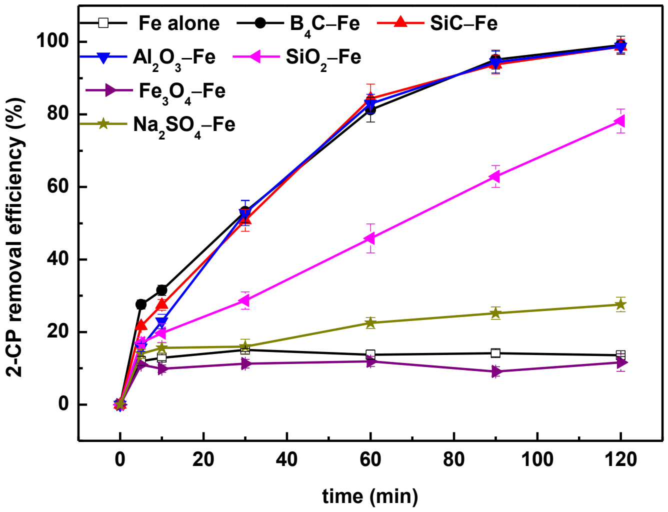

458

459 **Fig. 1.** The effect of different abrasives (100 mesh) on the removal of 50 ppm 2-CP in
460 aqueous solution at initial pH=3.0 using the dosage of 40 g/L. (milling conditions:
461 10% abrasive, 6% PCA, milling time = 3h)

462

463

464

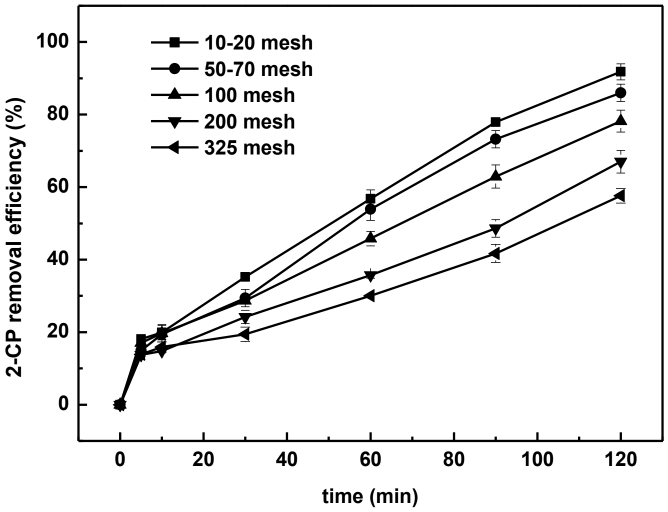

465

466 **Fig. 2.** The effect of SiO_2 size on the removal of 50 ppm 2-CP in aqueous solution at
467 initial pH=3.0 using 40 g/L SiO_2−Fe MMC. (milling conditions: 10% SiO_2, 6% PCA,
468 milling time = 3h)

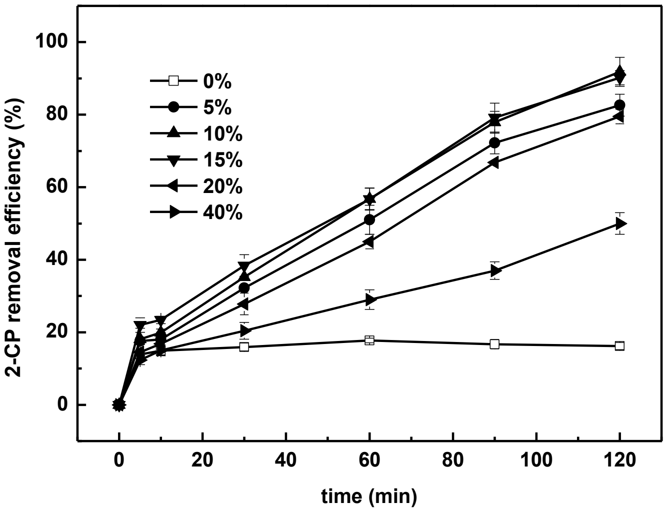

Fig. 3. The effect of SiO_2 dosage (10~20 mesh) on the removal of 50 ppm 2-CP in aqueous solution at initial pH=3.0 using 40 g/L SiO_2−Fe MMC. (milling conditions: 6% PCA, milling time = 3h)

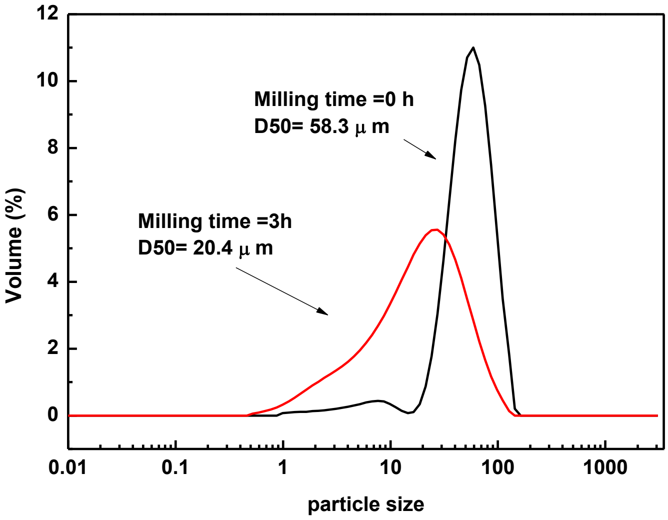

Fig. 4. The particle size distribution of the SiO_2−Fe MMC before and after ball milling for 3 h. (milling conditions: 10% SiO_2(10~20 mesh), 6% PCA, milling time = 3h)

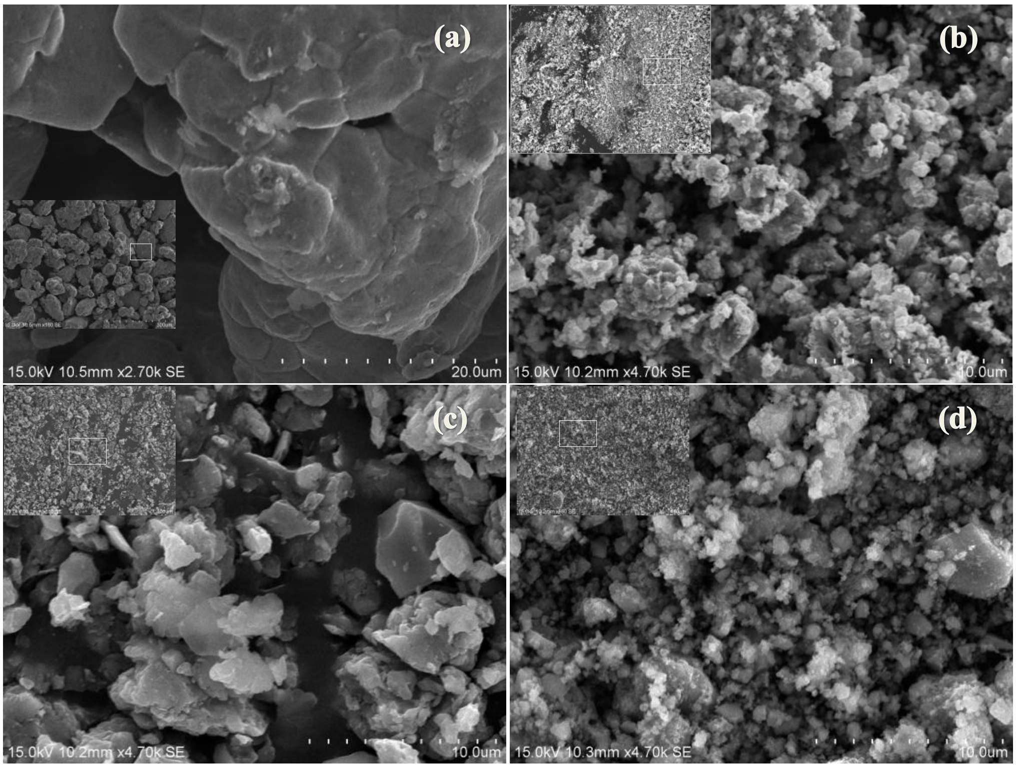

Fig. 5. SEM morphologies of the powders after milling for 3 h (a) the Fe alone, (b) SiO_2 and Fe, (c) SiO_2 and Al, (d) SiO_2 and Si. (milling conditions: 10% SiO_2(10~20 mesh), 6% PCA, milling time = 3h)

Table 1. The hardness of the different abrasives and the surface area of the milled abrasives−Fe MMCs. [a]

Name	Formula	S_{BET} (m^2/g)	Mohs scale hardness [23, 24]
Boron carbide	B_4C [b]	20.34	9.5
Silicon carbide	SiC [b]	20.21	9.3~9.5
Alpha-Alumina	α-Al_2O_3 [b]	19.94	9.0
Quartz sand	SiO_2 [b]	13.11	7.0
Magnetite	Fe_3O_4 [b]	3.18	6.0
Iron	Fe	2.81	4.0
Sodium	Na_2SO_4	2.90	2.8

sulfate

[a] milling conditions: 10% abrasives (100 mesh), milling for 3 h, milling speed=550 rpm.

[b] the size of abrasives used was 100 mesh.

Table 2. The effect milling time and PCA dosage on the dechlorination of 2-CP in aqueous solution using SiO_2−Fe MMC. [ab]

milling time (h)	PCA dosage (%, *w/w*)	Removal percent (%)
0	6	12.3
0.5		37.1
1		65.3
2		82.8
3		91.8
4		90.5
3	0	20.3
	1	45.5
	2	63.4
	4	86.5
	6	91.8
	8	65.3
	10	57.8

[a] Reaction conditions: SiO_2–Fe MMC dose = 40 g/L, initial pH=3.0, 2-CP concentration = 50 mg/L).

[b] milling conditions: 10% SiO_2 (100 mesh), milling for 3 h.

Table 3. The effect of metal categories on the dechlorination of 2-CP in aqueous solution using SiO_2−metal particles. [a]

Metal categories	t = 5min		t = 120 min		
	pH[b]	2-CP concentration (mM)	pH	2-CP concentration (mM)	phenol concentration (mM)
Al	5.35	0.342	5.53	0.340	ND[a]
Si	5.89	0.298	5.99	0.299	ND[a]
Fe	6.05	0.315	6.30	0.032	0.25

[a] Reaction conditions: SiO_2–metal MMC dose = 40 g/L, initial pH=3.0, 2-CP concentration = 50 mg/L).

[b] The pH meter (PHS-3C) was calibrated using buffers in aqueous solution. Buffer with pH values of 4.00 and 6.86 in water gave values of 4.01 and 6.83, respectively.

Graphical Abstract: